

A facile green synthesis of nanostructured Gold–Silver@Carbon (Au–Ag@C) nano catalyst and its applications

P. Kavitha¹, C. Shanthi^{1,*}, R. Kannan²

¹*Dept. of Physics, Sona College of Technology (Autonomous), Salem – 636 005, India.*

²*Dept. of Chemistry, Sri K.G.S. Arts College, Srivaikuntam – 628 612,*

Affiliated to Manonmaniam Sundaranar University, India.

**Corresponding author: shanthic@sonatech.ac.in*

Abstract

In this communication, the room-temperature synthesis of gold–silver nano-structures using ascorbic acid (AA) by simple one-step process is reported. Furthermore, the core–shell-type of gold–silver@carbon catalyst (Au–Ag@C) has been derived by microwave irradiation. The surface morphology expresses the neat single metal and bimetal formation. The AA acts as a reductant as well as a stabilizer of metal nanoparticles (MNPs). The microscopic studies reveal the formation of MNPs as quantum dots (~3–5 nm). The excess reductant has been used as a precursor for carbon and in some case it forms as nanowires. The catalyst Au–Ag@C shows the excellent catalytic activity toward 4-nitrophenol reduction at room temperature. The proposed method is facile, fast and eco-friendly for the synthesis of Au–Ag MNPs.

Keywords: Bimetallic; catalysis; core–shell; Gold–Silver nanoparticles; nanowire;

1. Introduction

Noble metals with nanostructures attract significant attention due to their potential applications in gas and biosensors, catalysis, energy storage, and conversion [Campelo JM, 2009; Narayan N, 2019; Khandel P, 2018; Gao Z, 2014]. Especially noble metals, such as, gold (Au), silver (Ag), platinum (Pt), and palladium (Pd), are widely used. In the recent past, enormous developments have been achieved in the field of nanoscience and technology. Along with this, numerous methods have been suggested to synthesize metal nanoparticles (MNPs) with the controlled size and shape because these characteristics such as size and shape, play a vital role towards the specific applications [Sasaki K, 2012; Fu S, 2015]. In addition, these MNPs have been developed using various reducing agents, but most of them are hazardous [Tabrizi NS, 2013] and are also inevitable to overcome eco-friendly methods that are highly needed.

MNPs, such as, Au, Ag, and Au–Ag NPs, have been prepared by several reducing agents, such as, sodium borohydride [Tabrizi NS, 2013], ascorbic acid (AA) [Boote BW, 2013; Kannan R, 2014], glycerol [Nawaz R, 2019], hydroquinone [Kumar D, 2016], polysaccharides [Banerjee A, 2017], etc. Among these reducing agents, AA plays a versatile role and acts as an excellent reducing agent. Recently, a number of research groups have studied the AA mediated reduction of

MNPs [Boote BW, 2013; Kannan R, 2014]. However, the complete reduction mechanism of MNPS is yet to be studied thoroughly.

Recent studies explain the formation of the MNPs [platinum (Pt), silver (Ag), and gold (Au)] using AA in an aqueous medium [Boote BW, 2013; Kannan R, 2014]. However, the AA has a strong affinity for the water molecules [Kannan R, 2016] resulting in a slow reduction process. In addition, the MNPs become aggregated into clusters in the aqueous medium [Ramasubbu A, 2000]. The high surface energy and strong interaction/attraction between these MNPs result in agglomeration or a change in shape during the catalysis reaction [Sasaki K, 2012; Fu S, 2015] and also proves that the catalytic ability is reduced due to the reduction of active catalytic sites. To overcome these difficulties, various methods have been suggested [Li C 2018, Li C 2018] and one of them is to place the MNPs with the suitable support [Li C 2018, Kannan R, 2015].

Boote *et al.*, have reported the one-pot synthesis of Ag–Au bimetallic NPs in the aqueous medium using L-AA as a reducing agent. These NPs are transformed into the large anisotropic structure by light irradiation with CTAB. This process yields Ag NPs size ranging from 15 to 40 nm core and Au shell of about 40 nm. In addition, the author has reported that the slow addition of Au solution results in the better formation of core–shell structure. This Ag core–Au shell nanostructure results in the improved optical property that can be tuned easily by light irradiation and the result exhibits a good application in the visible or near IR regions of the spectrum [Boote BW, 2013].

Additionally, Carbon, which is a very important catalyst support material, can be derived from different sources [Dutta S 2017, Wang J 2018]. This paper presents a simple strategy for *in situ* development of core–shell-type nanostructures of MNPs–carbon catalyst (MNPs@C) by the mechanochemical process with microwave heating. This results in the formation of 2–8 nm sized Au, Ag, Au–Ag NPs at room temperature. The detailed synthesis, formation mechanism, and the catalytic activity are reported in detail.

2. Experimental method

2.1. Materials

Ascorbic acid (AA) has been received from Alfa Aesar chemicals, Republic of Korea and Chloroauric acid and silver nitrate have been obtained from Sigma–Aldrich. Analytical grade chemicals have been purchased and used as received without further purification.

2.2. Room-temperature synthesis of Au–Ag–DHA nanowire

Equi-mixture of silver nitrate (10 mg) and Chloroauric acid (10 mg) is mixed with 40 mg of AA powder and grounded in the mortar for about 2–3 min. Then, the results of the solid were stored in glass vial for about one week. On the other hand, mono metal precursor (Au/Ag) was grounded with AA powder for about 2-3 min. Additionally, AA crystals were grounded without metal precursors and stored.

2.3. Synthesis of Carbocatalyst

Equi-mixture of silver nitrate (10 mg) and chloroauric acid (10 mg) is mixed with 40 mg of AA powder and grounded in the mortar for about 2–3 min and subjected to microwave irradiation using commercial microwave oven (Samsung, 2400 W) till the color of the sample turns black. (approx.20 min with regular interval of 30 sec.).

2.4. Characterization

The prepared catalysts are characterized using powder X-ray Diffraction (XRD, Rigaku Instrument diffractometer with Cu K_{α} radiation). The FTIR spectra are recorded on a Perkin Elmer (Spectra GX) spectrometer in the range of 400–4000 cm^{-1} and the Fourier Raman spectra are recorded using a Nano-finder 30 confocal Raman microscope (Tokyo Instrument Co., Japan) in the range of 500–3200 cm^{-1} with a He–Ne laser beam of 633 nm wavelength. The X-ray Photoelectron Spectra (XPS) are recorded on an Axis-Nova (Kratos Inc.) with an Al K_{α} =1486.6 eV excitation source. Furthermore, the characterization is performed by employing Field Emission Scanning Electron Microscopy (FE-SEM) equipped with the Energy Dispersive X-ray Spectrometer (EDS) for the quantitative determination of the elements present in the catalyst on a JEOL, JSM-6200 equipped with an Oxford instruments, at an accelerating voltage of 5–20 kV. The images from High Resolution Transmission Electron Microscopy (HRTEM) are recorded with JEOL, JEOL 2100 electron microscope operated at 200 kV.

2.5. Catalytic studies

About 1.6 mL of 4-nitrophenol (0.1 mmol L^{-1}) and aqueous solution of ice-cold NaBH_4 (0.10 mL of 0.10 mol L^{-1}) were added successively into a 4.5 mL long neck quartz cuvette. Subsequently, 20 mg of metal catalyst was dissolved into the above solution by shaking gently. The reduction reaction of 4-nitrophenol was characterized by its optical absorption spectrum every 300 s over the range from 200 to 500 nm and all the experiments of the conversion of 4-nitrophenol to 4-aminophenol were carried out under the same conditions.

3. Results and discussion

The crystal structures of Au–Ag@C and nanowires are characterized by powder X-ray technique shown in figure 1. The XRD peaks for Ag@C indicated in figure 1(d) and the characteristic peaks for Ag NPs are shown as peaks (2θ) at 37.1, 43.2, 63.6, and 76.8 corresponding to the Ag (111), (200), (220), and (311), respectively. In addition, the Au (111), (200), and (220) crystal planes are observed as (2θ) at 39.1, 44.2, and 65.3, respectively (figure 1(c)). The nanowires express insignificant XRD peaks, which indicate that the quantity of MNPs is comparatively smaller than the DHA; hence, amorphous peaks are observed. Figure 1(a) shows the XRD patterns of Au–Ag@C, where the peaks (2θ) at 39.1, 44.1, 65.2, and 79.1 correspond to Au–Ag (111), (200), (220), and (311), respectively. In all these, XRD peaks are shifted slightly from the original Au or Ag NPs peaks and this may be attributed to the carbogenous materials that interfere or alter the peaks [Malathi S, 2014; Francis S, 2017]. The particles of Au-Ag bimetallic nanoparticles based

on the scherrer formula of Au-Ag@C, Ag@C and Au@C are exhibited as 5.87, 5.65, 5.15 nm respectively.

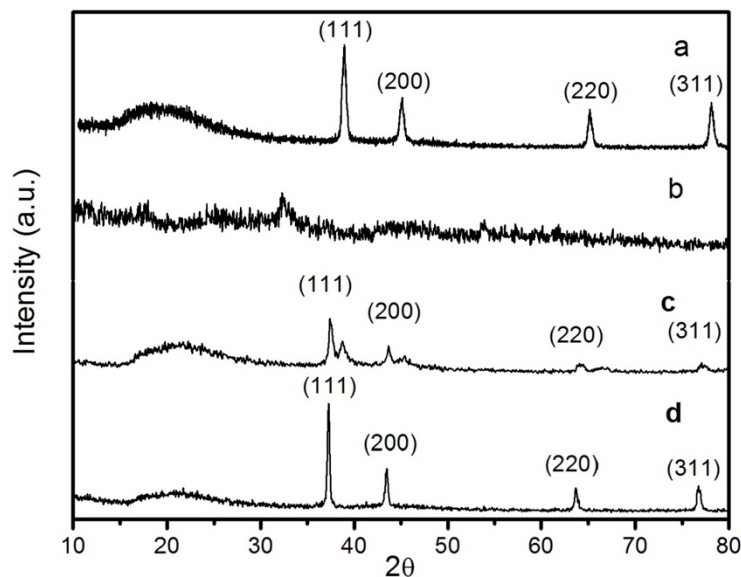


Fig. 1. Powder XRD profiles of (a) AuAg@C, (b) AuAg-nanowire, (c) Au@C and (d) Ag@C

The number of research reports reveals the reduction ability of AA toward the MNPs, especially, noble MNPs in the aqueous medium. However, in this medium, the MNPs become aggregated into cluster. To overcome this, Au–Ag MNPs are prepared at the room-temperature. The suitable quantities of metal precursors and AA are grounded in mortar for about 5–10 min. The color of the samples turns from pale yellow to brownish black. A part of the sample stored in glass vial and another part of the sample is heated in microwave for 10 minutes. The first part stored in glass vial is analyzed by TEM and the micrographs show the formation of beautiful nanowires, and the Au–Ag MNPs are uniformly distributed over these wires (figure 2). Both the mono-metal (Ag/Au) exhibit similar nanostructures. But, the AA crystals which were grounded without the metal precursors show an agglomerated microstructure. The results clearly show that the nanowires were formed only with the metals. The mechanism of the formation of Au–Ag nanowires is as follows: during the mechano-chemical process, the AA reduces the metal precursors (Au and/or Ag) which turn into dehydroascorbate (DHA). The DHA with the humidity (water in the air) undergoes aerial oxidation and transforms into nanowires encompassing MNPs. This process clearly explains that the AA acts as a reducing agent as well as a protecting group to restrict the agglomeration of MNPs. Hence, the MNPs retain its size and shape. On microwave heating, the DHA turns into carbon and the earlier study explains the formation of carbon from the AA-DHA [Kannan, 2015]. Additionally, in the presence of both mono and bimetal, carbon shell nanostructures have formed in the core through microwave heating process.

The surface morphology of nanowires and Au–Ag@C is shown in figure 2. The nanowires are uniformly arranged as web-like structure. The size ranges and higher magnification micrographs show that MNPs are embedded (Au–Ag) in the nano wires and the MNPs size range from 2 to 9 nm. The EDX micrograph confirms the presence of Au–Ag on the nanowires (figure 3). The microwave heated compounds, i.e., Au@C and Au–Ag@C, show the core–shell-like nanostructures. Figure 4 shows Au@C and it displays the single Au NPs covered with carbon very clearly. Similarly, the Au–Ag@C also shows the same kind of core–shell nanostructures (figure 4). However, Au–Ag covers up to five to six atoms assembled together in the core.

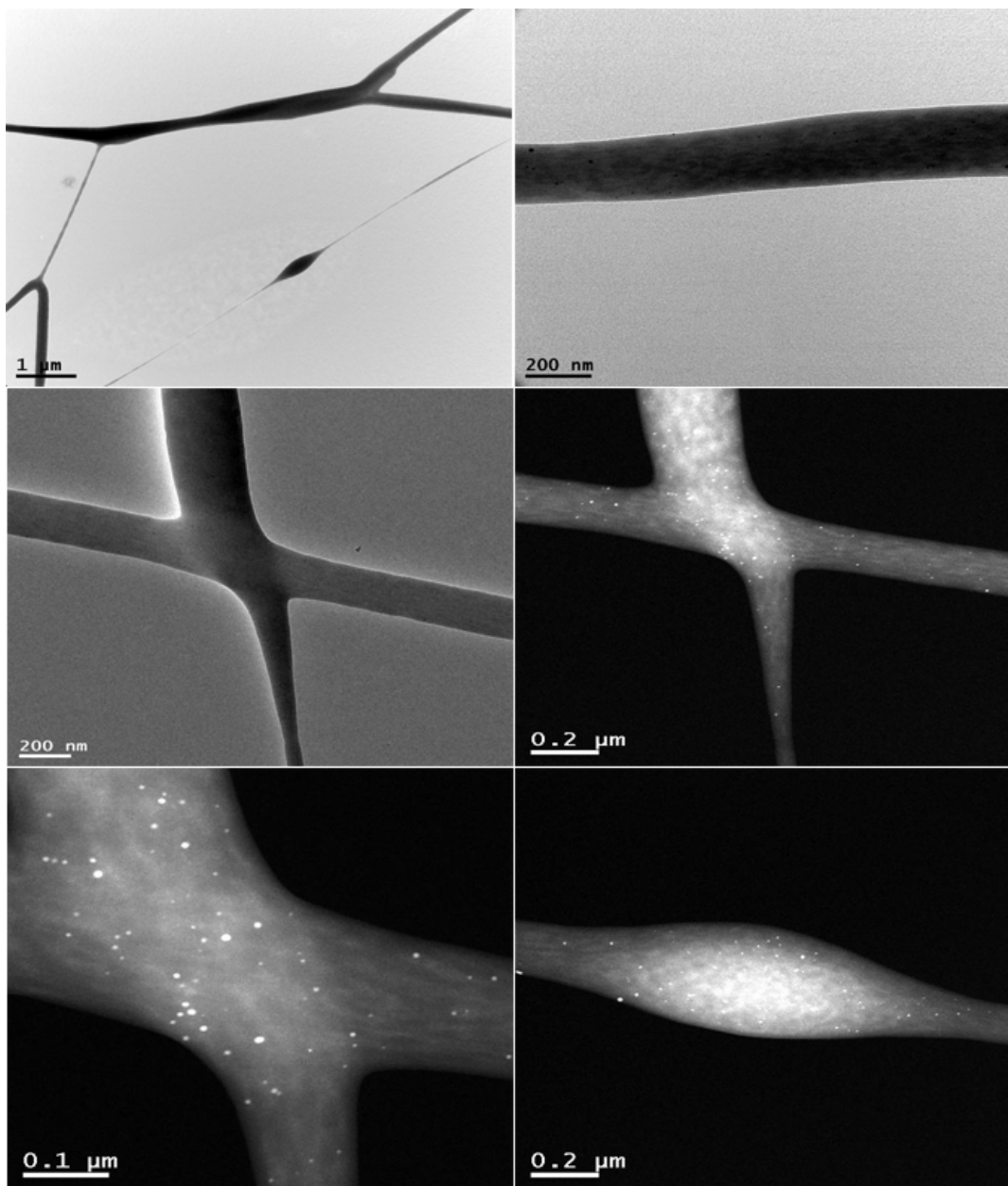


Fig. 2. TEM images of the AuAg nanoparticles in AA nanofibers prepared through solid state room temperature process.

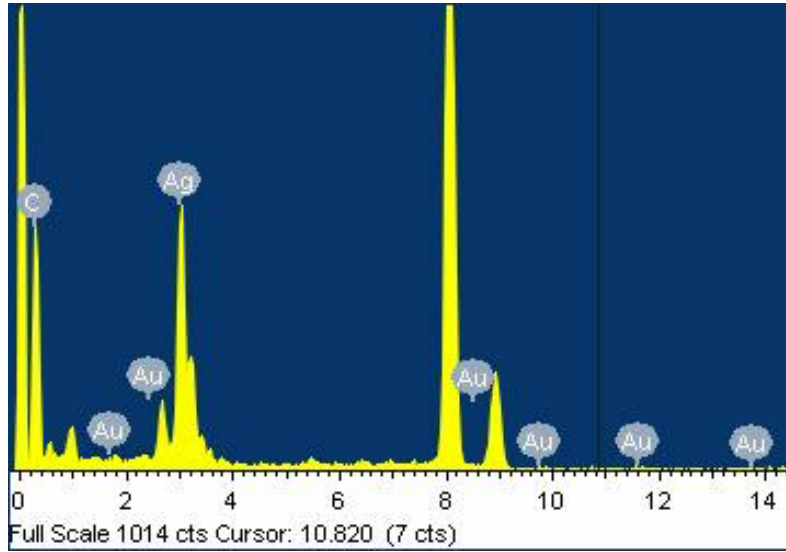


Fig. 3. EDX profile for AuAg@C

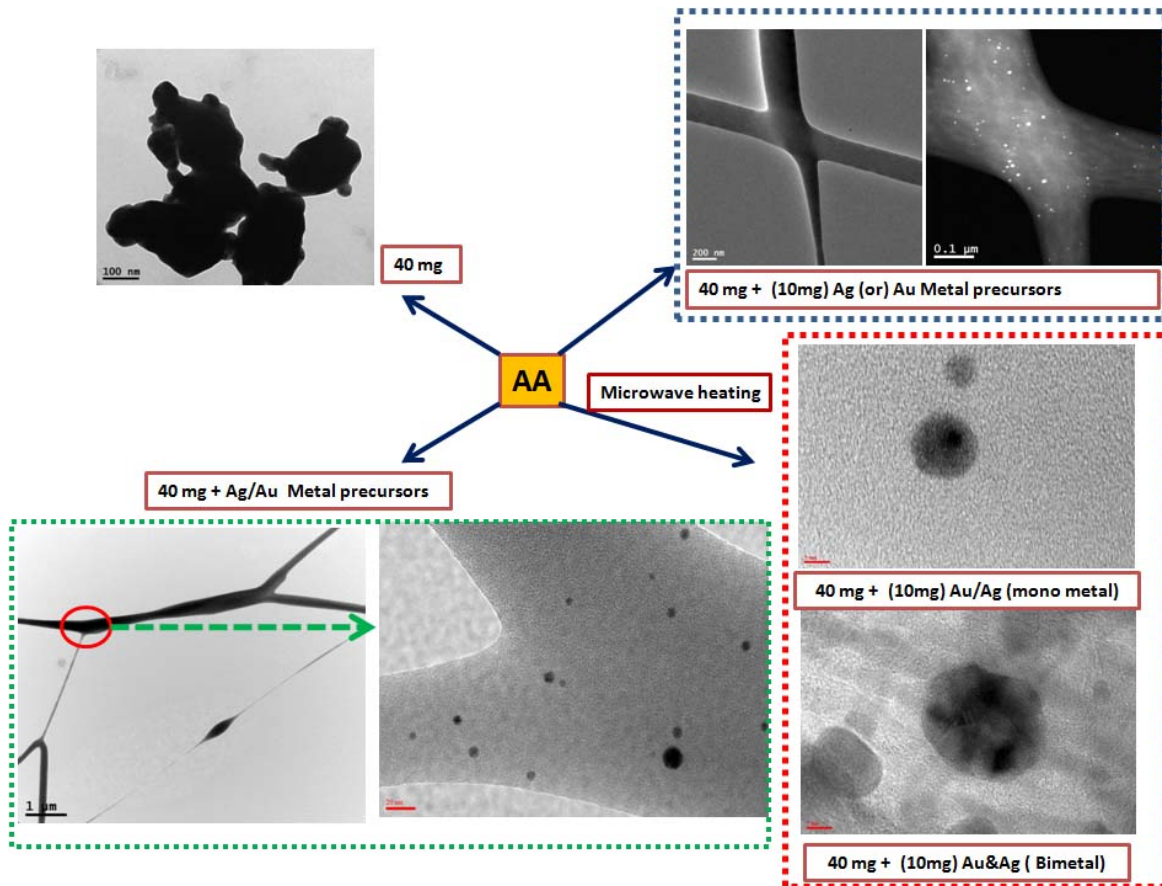


Fig. 4. TEM image of single Au nanoparticles @ carbon.

The evaluation of the formation of carbon material on MNPs is analyzed using FT–Raman. Figure 5 shows the FT–Raman micrograph for Ag@C and Ag–Au@C. In general, the carbon material exhibits two characteristic peaks, namely, G and D at 1359 and 1593 cm^{-1} , respectively [Kannan 2014]. The prepared samples, i.e., after microwave heating, show two characteristic peaks for Ag@C and Ag–Au@C of G and D, respectively. Thus, it proves that the shell material or carbon is similar to the graphitic one. The intensity ratio of D and G bands (I_D/I_G) for Ag@C and Ag–Au@C are 1.0738 and 0.9727, respectively, which indicate that the carbon materials in Ag@C form more defective structure compared to Ag–Au@C.

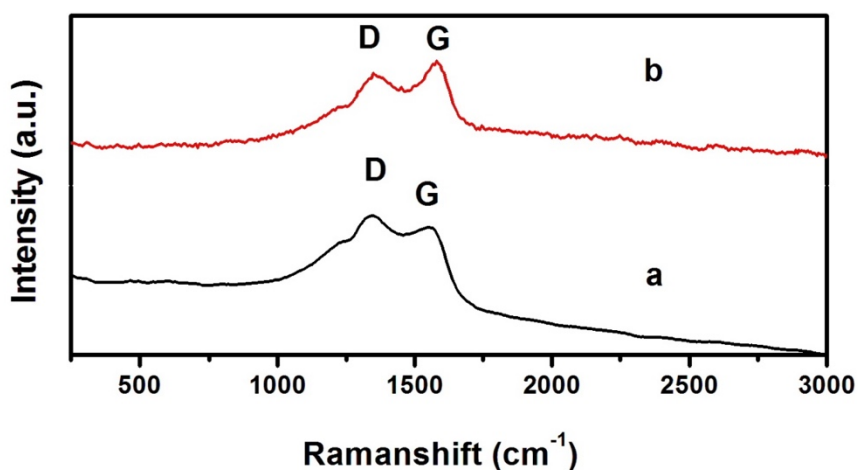


Fig. 5. Raman spectrum of (a) Ag@C and (b) AuAg@C nanostructures

The chemical state of the prepared Au–Ag@C is analyzed and figure 6 (a–d) shows the XPS spectra of the Au–Ag@C. Figure 7 (a) shows the binding energy of Au 4f_{7/2} and 4f_{5/2} at 83.8 and 87.5 eV, respectively, which corresponds to the gold NPs. Furthermore, Ag 3d_{3/2} and Ag3d_{5/2} at 374.1 and 385.2 eV, respectively, correspond to silver NPs. In addition, figure 7 (d) exhibits the peak at *ca.* 284.3 eV corresponding to the binding energy of C1s that is further deconvoluted into two peaks at 286.3 and 282.2 eV, which correspond to C–C/C=C, C–O, and M–C–O, respectively [Kannan R, 2014; Vitale F, 2011; Ding W, 2014]. The above results clearly indicate the formation of Au–Ag@C.

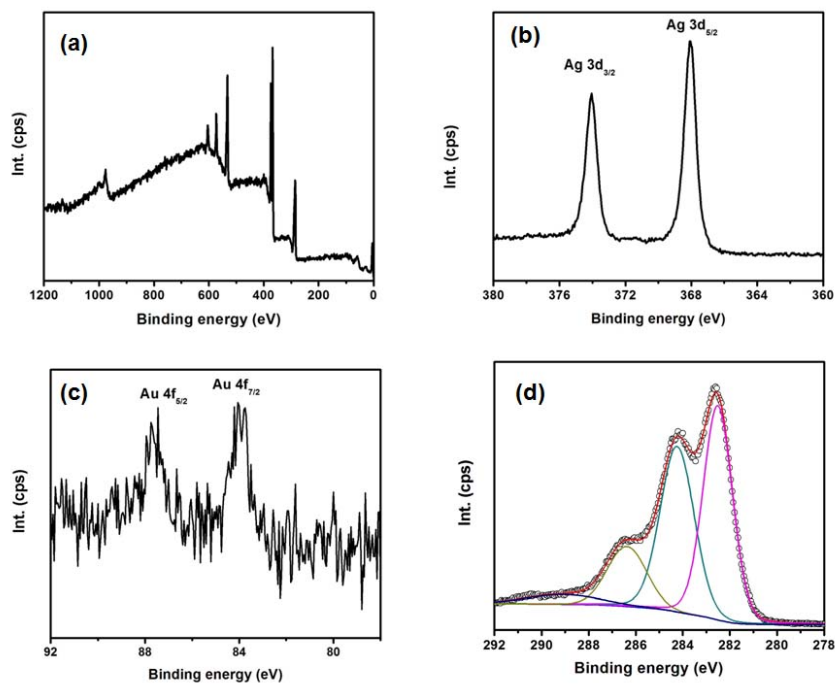


Fig. 6. XPS profile of AuAg@C; (a) survey, (b) Ag 3d, (c) Au 4f and (d) C 1s spectrum.

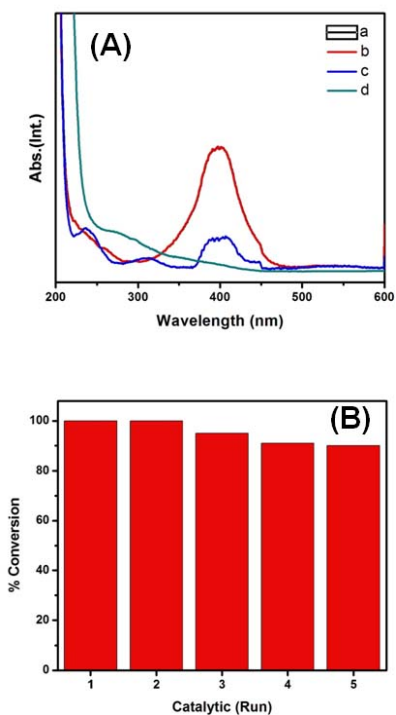


Fig. 7. (A) UV-Vis. Spectrum of (a) blank 4-NP, (b) 4-NP+NaBH₄, (c) Nanowire and (d) AuAg@C catalyzed 4-NP to 4-AP, (B) Catalytic efficacy (number of runs) for the conversion of 4-NP to 4-AP.

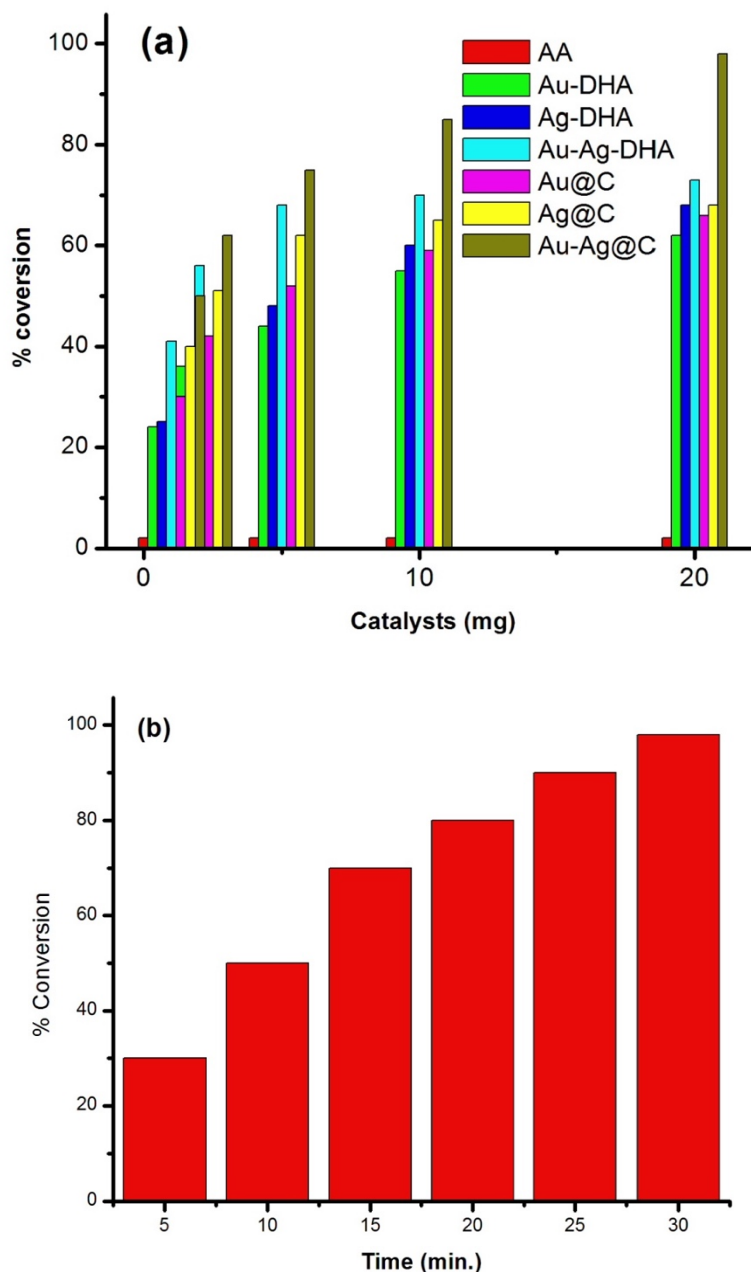


Fig. 8. Catalytic studies of Au–Ag@C on the conversion of 4-NP to 4-AP.

The catalytic activity of prepared Au–Ag@C is tested for the catalytic reduction of 4-nitrophenol (4-NP, $1 \times 10^{-5} \text{ M}$) to 4-amino phenol (4-AP) in the presence of sodium borohydride (NaBH_4 , $0.5 \times 10^{-5} \text{ M}$). The Au–Ag@C catalyst exhibits excellent catalytic activity for the reduction of 4-NP to 4-AP in 10 s. Figure 7A, (a) and (b) indicate the 4-NP before and after the addition of reducing agent without catalyst, respectively; it also indicates that no obvious changes in the peak are observed; and no characteristic reaction are found to occur, i.e., no reduction is observed. Then, 25 mg of nanowire (Au–Ag) catalyst introduced into the reaction. The resultant 4-AP formation is

observed clearly by the diminished peak at 400 nm and the characteristic absorption peak for 4-AP is observed around 310 nm (figure 8). From this, it is understood that the catalyst plays a vital role in the transformation/reduction of 4-NP to 4-AP. Figure 7(A), (a)–(d) show no characteristic peaks of 4-NP that is observed, and it indicates that the complete reduction of 4-NP occurs with the Au–Ag@C catalyst. It also indicates that after the heat treatment, the catalyst is more active. In addition, slight shift in peaks is observed and it is due to the associated plasmonic adsorption of 4-AP and Au–AgNPs. The reuse of the catalyst shows good catalytic activity and after five tests, the catalytic activity reduces by 9% and stability holds good (figure 7(B)). The catalytic efficacy on the conversion of 4-NP to 4-AP was tested with different catalyst at different amount of catalyst (1 mg, 2 mg, 5 mg, 10 mg and 20 mg, (figure 8a) such as mono Au, Ag and Au-Ag nano particles with DHA with nanostructured Au@C, Ag@C, and Au-Ag@C. Experimental results among the different catalyst Au-Ag@C showed excellent catalytic efficacy. Additionally, the catalyst response against the reaction time was measured and after 30 min (figure 8b) of the reaction, about 98% conversion was observed. The best results observed was at 20 mg Au-Ag@C which was about 98% at 30 min. A detailed catalytic activity towards other pollutants such as organic dyes and their interaction towards biomedical applications are in progress.

4. Conclusion

This research work demonstrates the synchronized one-pot quick synthesis of the Au–Ag MNPs by solid-state process using AA as an eco-friendly reducing agent at room temperature. The solid-state reduction process yields nanofibrous dehydroascorbate nanowire embedded with Au–Ag MNPs. Furthermore, on heating, a core–shell type of Au–Ag core and carbon–shell-like nanostructures are obtained. The AA plays bi-functional role, namely, reducing agent and surface protecting agent. In addition, the prepared catalyst exhibits excellent catalytic activity towards the reduction of 4-nitrophenol to 4-aminophenol. The proposed technique is a facile, fast, and eco-friendly method for the synthesis of the Au–Ag MNPs and also for environmental applications.

References

- Banerjee, A., Halder, U. & Bandopadhyay R. (2017)** Preparations and applications of polysaccharide based green synthesized metal nanoparticles: A state-of-the-art, *Journal of Cluster Science*, 28:1803-1813.
- Boote, BW., Byun, H. & Kim, JH. (2013)** One-pot synthesis of various Ag-Au bimetallic nanoparticles with tunable absorption properties at room temperature, *Gold Bulletin*, 46:185-193.
- Campelo, JM., Luque, D., Luque, R., Marinas, JM. & Romero, AA. (2009)** Sustainable preparation of supported metal and their applications in catalysis, *ChemSusChem.*, 2:18-45.
- Ding, W., Liu, Y., Li, Y., Shai, Q., Li, H., Xia, H., Wang, D. & Tao X. (2014)** Water-soluble gold nanocluster with pH-dependent fluorescence and high colloidal stability over a wide pH range via co-reduction of glutathione and citrate, *RSC Advances*, 4:22651-22660.

Dutta, S., Kim, J., Ide, Y., Kim, JH., Hossain, MDA., Bando, Y., Yamauchi, Y., Wu. & KCW. (2017) 3D network of cellulose-based energy storage devices and related emerging applications, *Materials Horizons*, 4:522-545.

Francis, S., Joseph, S., Koshy, EP. & Mathew, B. (2017) Synthesis and characterization of multifunctional gold and silver nanoparticles using leaf extract of naregaminaalata and their applications in the catalysis and mastitis, *New Journal of Chemistry*, 41:14288-14298.

Fu, S., Zhu, C., Du, D. & Lin, Y. (2015) Facile one-step synthesis of three-dimensional Pd-Ag bimetallic alloy networks and their electrocatalytic activity towards ethanol oxidation, *ACS Applied Materials & Interfaces*, 7:13842-13848.

Gao, Z., Su, R., Huang, R., Qi, W. & He, Z. (2014) Glucomannan-mediated facile synthesis of gold nanoparticles for catalytic reduction of 4-nitrophenol, *Nanoscale Research Letters*, 9:404-412.

Kannan, R., Jang, HR., Yoo, ES., Lee, HK. & Yoo, DJ. (2015) Facile green synthesis of palladium quantum dots@Carbon on mixed valence cerium oxide/graphene hybrid nanostructured bifunctional catalyst for electrocatalysis of alcohol and water, *RSC Advances*, 5:35993-36000.

Kannan, R., Kim, AR., Nahm, KS., Lee, HK. & Yoo, DJ. (2014) Synchronized synthesis of Pd@C-RGOCarbocatalyst for improved anode and cathode performance for direct ethylene glycol fuel cell. *Chemical Communications*, 50:14623-14626.

Kannan, R., Kim, AR., Nahm, KS. & Yoo, DJ. (2016) Facile instep synthesis of palladium nanoparticles/carbon@cabon nanotube composites for electrooxidation of xylitol, *Journal of Nanoscience and Nanotechnology*, 16:2587-2592.

Khandel, P., Yadaw, RK., Soni, DK., Kanwar, L., Shahi, SK. (2018) Biogenesis of metal nanoparticles and their pharmacological applications: present status and application prospects, *Journal of Nanostructure in Chemistry*, 8:217-254.

Kumar, D., Mutreja, I., Sykes, P. (2016) Seed mediated synthesis of highly mono-dispersed gold nanoparticles in the presence of hydroquinone, *Nanotechnology*, 27(35):355601.

Li, C., Iqbal, M., Lin, J., Luo, X., Jiang, B., Malgras, V., Wu, KCW., Kim, J. & Yamauchi, Y. (2018) Electrochemical deposition: An advanced approach for template synthesis of nanoporous metal architectures, *Accounts of Chemical Research*, 51:1764-1773.

Li, C., Tan, H., Lin, J., Luo, X., Wang, S., You, J., Kang, YM., Bando, Y., Yamauchi, Y., & Kim, J. (2018) Emerging Pt- based electrocatalysts with highly open nanoarchitectures for boosting oxygen reduction reaction. *Nano Today*, 21:91-105.

Malathi, S., Ezhilarasu, T., Abiraman, T. & Balasubramanian, S. (2014) One pot green synthesis of Ag, Au and Au-Ag alloy nanoparticles using isonicotinic acid hydrazide and starch, *Carbohydrate Polymers*, 111:734-743.

Narayan, N., Meiyazhagan, A. & Vajtai R. (2019) Metal nanoparticles as green catalysts. *Materials*, 12:3601-3612.

Nawaz, R., Kait, CF., Chia, HY., Isa, MH. & Huei, LW. (2019) Glycerol-mediated facile synthesis of colored titania nanoparticles for visible light photodegradation of phenolic compounds, *Nanomaterials*, 9:1585-1605.

Ramasubbu, A., Vanangamudi, A., Muthusubramanian, S., Ramachandran, MS. & Sivasubramanian, S. (2000) Electrocatalytic studies using silver-clay composite - a novel material, *Electrochemistry Communicatins*, 2:56-64.

Sasaki, K., Naohara, H., Choi, Y., Cai, Y., Chen, WF., Liu, P. & Adzic, RR. (2012) Highly stable Pt monolayer on PdAu nanoparticles electrocatalysts for the oxygen reduction, *Nature Communications*, 3:1-9.

Tabrizi, NS., Tazikeh, M. & Shahgholi, N. (2013) Antibacterial properties of Au-Ag alloy nanoparticles. *International Journal of Green Nanotechnology*, 4:489-494.

Vitale, F., Fratoddi, I., Battocchio, C., Piscopiello, E., Tapfer, L., Russo, MV., Polzonetti, G. & Giannini, C. (2011) Mono- and bi- functional arenethils as surfactants for gold nanoparticles: Synthesis and characterization. *Nanoscale Research Letters*, 6:102-110.

Wang, J., Xu, Y., Ding, B., Chang, Z., Zhang, X., Yamachi, Y. & Wu, KCW. (2018) Confined self-assembly in two-dimensional interlayer space: Monolayered mesoporous carbon nanosheets with in-plane orderly arranged mesopores and a highly graphitized framework. *Angewandte Chemie International*, 57(11):2894-2898.

Submitted: 22/02/2021

Revised: 28/06/2021

Accepted: 04/07/2021

DOI: 10.48129/kjs.12649